0026-895X/06/7003-1022–1032$20.00
MOLECULAR PHARMACOLOGY
Copyright © 2006 The American Society for Pharmacology and Experimental Therapeutics
Mol Pharmacol 70:1022–1032, 2006

Vol. 70, No. 3
24042/3135538
Printed in U.S.A.

Equilibrium Constants for (*R*)-[(*S*)-1-(4-Bromo-phenyl)-ethylamino]-(2,3-dioxo-1,2,3,4-tetrahydroquinoxalin-5-yl)-methyl]-phosphonic Acid (NVP-AAM077) Acting at Recombinant NR1/NR2A and NR1/NR2B *N*-Methyl-D-aspartate Receptors: Implications for Studies of Synaptic Transmission[S]

Pamela A. Frizelle, Philip E. Chen, and David J. A. Wyllie

Centre for Neuroscience Research, University of Edinburgh, Edinburgh, United Kingdom

Received March 30, 2006; accepted June 15, 2006

ABSTRACT

We have quantified the effects of the *N*-methyl-D-aspartate (NMDA) receptor antagonist (*R*)-[(*S*)-1-(4-bromo-phenyl)-ethylamino]-(2,3-dioxo-1,2,3,4-tetrahydroquinoxalin-5-yl)-methyl]-phosphonic acid (NVP-AAM077) at rat recombinant *N*-methyl-D-aspartate receptor (NR)1/NR2A and NR1/NR2B NMDA receptors expressed in *Xenopus laevis* oocytes. We observed no difference in the steady-state levels of inhibition produced by NVP-AAM077 when it was either preapplied or coapplied with glutamate. The IC_{50} values for NVP-AAM077 acting at NR1/NR2A NMDA receptors were, as expected, dependent on the glutamate concentration used to evoke responses, being 31 ± 2 nM (with glutamate at its EC_{50} concentration) and 214 ± 10 nM (at 10 times the EC_{50} concentration). Schild analysis confirmed that the antagonism produced by NVP-AAM077 at NR1/NR2A NMDA receptors was competitive and gave an estimate of its equilibrium constant (K_B) of 15 ± 2 nM. Furthermore, Schild analysis of an NMDA receptor carrying a threonine-to-alanine point mutation in the NR2A ligand binding site indicated that NVP-AAM077 still acted in a competitive manner but with its K_B increased by around 15-fold. At NR1/NR2B NMDA receptors, NVP-AAM077 displayed reduced potency. An IC_{50} value of 215 ± 13 nM was obtained in the presence of the EC_{50} concentration of glutamate (1.5 μM), whereas a value of 2.2 ± 0.14 μM was obtained with higher (15 μM) glutamate concentrations. Schild analysis gave a K_B for NVP-AAM077 at NR2B-containing receptors of 78 ± 3 nM. Finally, using a kinetic scheme to model "synaptic-like" activation of NMDA receptors, we show that the difference in the equilibrium constants for NVP-AAM077 is not sufficient to discriminate between NR2A-containing or NR2B-containing NMDA receptors.

The majority of NMDA receptors in the mammalian central nervous system are heteromeric assemblies made up of two NR1 and two NR2 subunits. NR1 subunits, which exist in one of eight splice variants, contain the binding site for the coagonist glycine, whereas four types of NR2 subunits exist (named NR2A–NR2D) and contain the binding site for glutamate (for reviews, see Dingledine et al., 1999; Erreger et al., 2004; Chen and Wyllie, 2006). By studying recombinant receptors of known subunit compositions, a defining "fingerprint" of their single-channel properties, deactivation kinetics, sensitivity to block by ions, and pharmacological sensitivity to a variety of agonists and antagonists can be obtained (Monyer et al., 1992, 1994; Ishii et al., 1993; Williams, 1993; Vicini et al., 1998; Wyllie et al., 1998; Erreger et al., 2004). Such information is invaluable when trying to identify the subunit composition of native NMDA receptors in central neurons. Unfortunately, it is rarely possible to undertake a series of biophysical-type experiments to identify the native NMDA receptor population; therefore, the development of selective antagonists that allow the unequivocal

This work was supported by Biotechnology and Biological Sciences Research Council grant BB/D001978/1 and funding from the Undergraduate Pharmacology Honours programme at the University of Edinburgh.

Article, publication date, and citation information can be found at http://molpharm.aspetjournals.org.

doi:10.1124/mol.106.024042.

[S] The online version of this article (available at http://molpharm.aspetjournals.org) contains supplemental material.

ABBREVIATIONS: NMDA, *N*-methyl-D-aspartate; NR, *N*-methyl-D-aspartate receptor; Ro 25-6981, *R*-(*R**,*S**)-α-(4-hydroxyphenyl)-β-methyl-4-(phenylmethyl)-1-piperidine propranol; CP 101,606, (1*S*,2*S*)-1-(4-hydroxyphenyl)-2-(4-hydroxy-4-phenylpiperidino)-1-propanol; NVP-AAM077, (*R*)-[(*S*)-1-(4-bromo-phenyl)-ethylamino]-(2,3-dioxo-1,2,3,4-tetrahydroquinoxalin-5-yl)-methyl]-phosphonic acid; TEVC, two-electrode voltage clamp; D-AP5, D-2-amino-5-phosphonopentanoic acid; EPSC, excitatory postsynaptic current; simEPSC, simulated excitatory postsynaptic current.

discrimination of NMDA receptor subtypes is extremely desirable.

Noncompetitive antagonists such as ifenprodil (Williams, 1993), Ro 25-6981 (Fischer et al., 1997), and CP 101,606 (Mott et al., 1998) display a selectivity for NR1/NR2B that is sufficient (> 200-fold) to allow these antagonists to be used to identify such receptors in native neurons. The competitive antagonist 1-(phenanthrene-2-carbonyl) piperazine-2,3-dicarboxylic acid has been reported to show modest selectivity for NR2C-containing and NR2D-containing NMDA receptors (Feng et al., 2004). As for NR1/NR2A receptors, the 5-phosphonomethylquinoxalinedione derivative, (*R*)-[(*S*)-1-(4-bromo-phenyl)-ethylamino]-(2,3-dioxo-1,2,3,4-tetrahydroquinoxalin-5-yl)-methyl]-phosphonic acid (NVP-AAM077) has been suggested to display a strong (>100-fold) selectivity for this receptor subtype compared with NR2B-containing receptors (Auberson et al., 2002; Liu et al., 2004). From these studies (where IC_{50} measurements were made), many investigators have used the values reported to support and justify their use of NVP-AAM077 as a selective antagonist of NR2A-containing NMDA receptors and to determine the roles played by native NMDA receptor subtypes in vivo and in vitro (Liu et al., 2004; Massey et al., 2004; Mallon et al., 2005; Toyoda et al., 2005; Barker et al., 2006; Kinney et al., 2006; Li et al., 2006). Recent reports, however, have claimed that the selectivity of this antagonist is not as great as first suggested, which may indicate that NVP-AAM077 cannot distinguish, in pharmacological terms, different NMDA receptor subtypes (Berberich et al., 2005; Weitlauf et al., 2005; Neyton and Paoletti, 2006).

In our study, we have quantified the actions of NVP-AAM077 at rat recombinant NR1/NR2A and NR1/NR2B NMDA receptors. We have compared its actions under conditions where NR1/NR2A and NR1/NR2B NMDA receptors are activated to the same extent by glutamate and have determined, using Schild analysis, equilibrium constants for NVP-AAM077 at these two receptor subtypes. In this study, we show why the translation of IC_{50} values to their use in studies of synaptic function is predicted to result in substantial block of both NR1/NR2A and NR1/NR2B NMDA receptors. Thus, although our data show that NVP-AAM077 is indeed more potent at NR1/NR2A compared with NR1/NR2B NMDA receptors, the extent of this selectivity is only approximately 5-fold. Moreover, the potency of NVP-AAM077 at both NR1/NR2A and NR1/NR2B NMDA receptors is such that during synaptic transmission this antagonist can be considered to act in an irreversible manner.

Materials and Methods

Plasmid Constructs, cRNA Synthesis, and Receptor Expression in Oocytes. The pSP64T-derived expression plasmids for rat NR1-1a (excluding exon 5, including exons 21 and 22, which we refer to as NR1) and wild-type NR2A, NR2A(S670G), and NR2A(T671A) NMDA receptor subunits have been described in Chen et al. (2005). The cDNA construct containing the wild-type rat NR2B subunit (NR2B pBS TR) was a gift from Dr. Stephen Traynelis (Emory University, Atlanta, GA). cRNA was synthesized as runoff transcripts from Mlu I (NR1 and NR2A) or NotI (NR2B)-linearized plasmid DNA using either the SP6 (NR1 and NR2A) or T7 (NR2B) polymerase RiboMax RNA synthesis kit (Promega, Madison, WI). Reactions were supplemented with 0.75 mM capping nucleotide, $m^7G(5')ppp(5')G$ (Promega) in the presence of 1.6 mM GTP. Integrity and yield of each synthesized cRNA was verified by fluorescence intensity in ethidium bromide-stained agarose gels. For recombinant NMDA receptor expression, NR1 and one of either the NR2A, NR2A(S670G), NR2A(T671A), or NR2B cRNAs were mixed at a nominal ratio of 1:1 and diluted with nuclease-free water to 5 ng/μl, before injection.

After administration of a lethal dose of anesthetic, oocytes were removed from *Xenopus laevis* (all procedures were carried out in accordance with current UK Home Office requirements). The follicular membranes of the oocytes were removed, oocytes were injected with cRNAs of interest, and individual oocytes were placed in separate wells of 24-well plates containing a modified Barth's solution with composition 88 mM NaCl, 1 mM KCl, 2.4 mM $NaHCO_3$, 0.82 mM $MgCl_2$, 0.77 mM $CaCl_2$, and 15 mM Tris-Cl, adjusted to pH 7.35 with NaOH (Sigma Chemical, Poole, Dorset, UK). This solution was supplemented with 50 IU/ml penicillin and 50 mg/ml streptomycin (Invitrogen, Paisley, UK). Oocytes were placed in an incubator (19°C) for 24 to 48 h to allow for receptor expression and then stored at 4°C until they were used for electrophysiological measurements.

Electrophysiological Recordings and Solutions. Two-electrode voltage-clamp (TEVC) recordings were made, using a GeneClamp 500 amplifier (Molecular Devices, Union City, CA), from oocytes that were placed in a modified frog Ringer's solution that contained 115 mM NaCl, 2.5 mM KCl, 10 mM HEPES, 1.8 mM $BaCl_2$, and 0.01 mM EDTA, pH 7.3 with NaOH (20°C) (Sigma Chemical). Current and voltage electrodes were made from thin-walled borosilicate glass (GC150TF-7.5; Harvard Apparatus, Kent, UK) using a PP-830 electrode puller (Narishige, Tokyo, Japan) and when filled with 3 M KCl possessed resistances of between 0.5 and 1.5 MΩ. Oocytes were voltage-clamped at potentials of between −20 and −60 mV so as to ensure that the currents generated after the application of agonist were generally <3 μA. Test solutions were applied for 20 s or until a plateau to the agonist-evoked response had been achieved. Application of solutions was controlled manually, and data were filtered at 10 Hz and digitized at 100 Hz. All glutamate-containing solutions were supplemented with a saturating concentration of glycine (50 μM) to ensure the coagonist binding site on the NR1 receptor subunit was fully occupied. NVP-AAM077 was kindly supplied by Dr. Yves Auberson (Novartis Institutes for Biomedical Research, Basel, Switzerland).

Data Analysis for Concentration-Response Curves. To determine the concentration of NVP-AAM077 required to inhibit glutamate-evoked responses by 50% (IC_{50}), the following procedures were adopted. For both NR1/NR2A and NR1/NR2B NMDA receptors, glutamate concentrations were set to give 50% of a maximal response (EC_{50}) or 10 times this concentration. Thus, two IC_{50} values were determined for each receptor subtype. Inhibition curves for NVP-AAM077 were fitted individually for each oocyte with the equation $I = I_{[B]0}/(1 + ([B]/IC_{50})^{nH})$, where n_H is the Hill coefficient, $I_{[B]0}$ is the current in the absence of antagonist, and [B] is the concentration of the antagonist. Each data point was then normalized to the fitted maximum of the dose-response curve. The normalized values were then pooled and averaged for each construct and fitted again with this same equation, with the maximum and minimum for each curve being constrained to asymptote to 1 and 0, respectively.

Because we had no data from our laboratory concerning the actions of glutamate at NR1/NR2B NMDA receptors, we determined its EC_{50} concentration under our recordings. Dose-response curves were fitted individually for each oocyte with the Hill equation $I = I_{max}/(1 + (EC_{50}/[A])^{nH})$, where I_{max} is the predicted maximum current and [A] is the agonist concentration. Again, we normalized data points to the fitted maximum, before refitting averaged data sets.

Schild Analysis. NVP-AAM077 antagonism was examined by the Schild method (Arunlakshana and Schild, 1959; also see Anson et al., 1998). Dose ratios from individual oocytes were determined at low agonist concentrations as follows. First, a partial concentration-response curve was generated from currents induced by two concentrations ($\ll EC_{50}$) of agonist in the absence of antagonist. Next,

partial concentration-response curves in the presence of a series of increasing NVP-AAM077 concentrations were obtained by applying higher concentrations of glutamate so as to produce approximately equivalent responses. Each NVP-AAM077 concentration was preapplied for 120 s before obtaining responses to glutamate. Each series of two-point concentration-response curves was plotted on a log-log scale, because the low concentration limit of the Hill equation gives a straight line in such plots. The slope of the line used to fit the initial (antagonist-free) two-point concentration-response curve was used to fit the remaining curves, thus generating a series of parallel lines in the presence of increasing NVP-AAM077 concentrations. These parallel fits were used to calculate the dose ratio (r, defined as the ratio of the glutamate concentrations needed to produce the same response in the presence and absence of NVP-AAM077) for each antagonist concentration used. The mean dose ratios for each concentration of NVP-AAM077 were used to construct a Schild plot, of log $(r - 1)$ versus log [B], where [B] is the antagonist concentration. This plot was initially fitted with a straight line with an unconstrained slope. The slope of the Schild plot is predicted by the Schild equation to be unity for a competitive antagonist at equilibrium. Thus, if the slope of the "free" fit was sufficiently close to 1, then the results were to be taken to be consistent with the Schild equation, and the data were refitted with the slope fixed at 1; i.e., they were refitted with the Schild equation $(r - 1) = [B]/K_B$ in which the only free parameter is the intercept on the x-axis and which is equal to the log of the equilibrium constant for antagonist binding, K_B.

Simulation of Synaptic Currents. Simulation of synaptic currents was performed using Channelab (http://www.pharm.emory.edu/traynelis/Downloads). The kinetic scheme used to model NR1/NR2A and NR1/NR2B NMDA receptor currents was as described previously and used the rate constants appropriate for the particular NR2 subunit (Erreger et al., 2005a). The kinetic scheme used contains no explicit binding (and unbinding) of glycine to the NR1 subunit, because we assumed these sites to be fully occupied. Numerical integration (fourth order Runga Kutta with a step size of 2.5 μs) was used to evaluate the occupancies of each state in the kinetic scheme. We approximated the concentration change produced in the synaptic cleft during glutamatergic synaptic transmission as an instantaneous step change in the glutamate concentration from zero to 10 mM (duration of 1 ms). For the simulation of NMDA currents produced during tetanic stimulation Monte-Carlo simulations were used to predict the action of glutamate (in the presence or absence of NVP-AAM077) on a population of 1000 channels (at a resolution of 50 kHz, filtered at 2 kHz for display purposes). The same step change in glutamate levels were used but repeated at intervals of 10 ms (equivalent to 100-Hz tetanus) for a duration of 0.5 s.

Statistical Analysis. Two-tailed Student's t tests (paired, where appropriate) were used to assess differences between means with statistical significance being taken at the $p < 0.05$ level. Results are expressed as mean ± S.E.M.

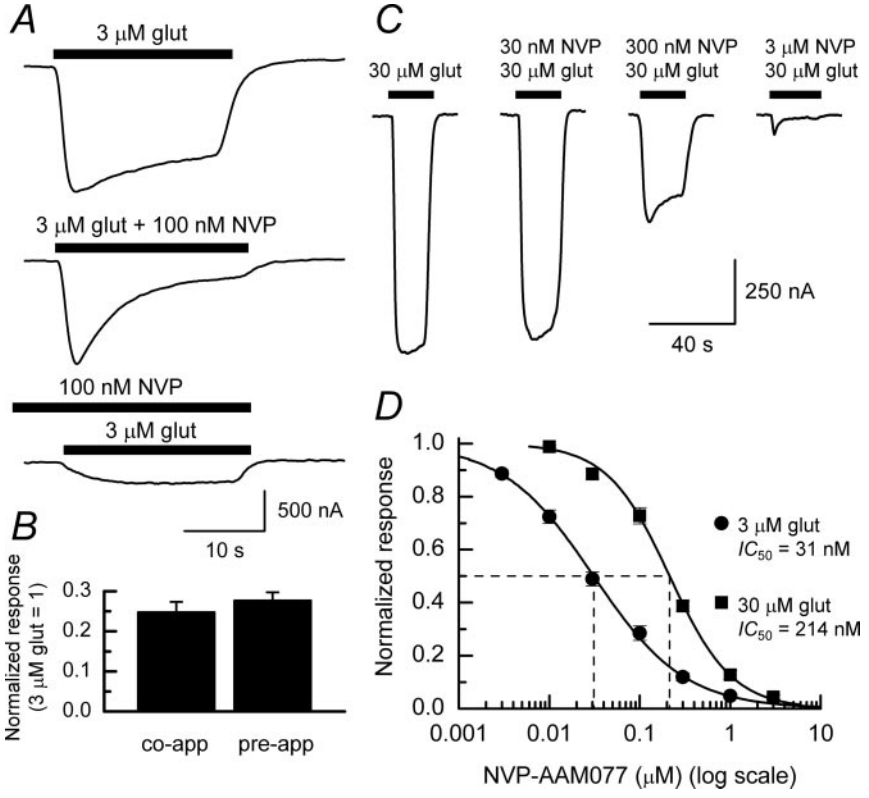

Fig. 1. Characterization of NVP-AAM077 antagonism at NR1/NR2A NMDA receptors. A, TEVC responses obtained from an oocyte (voltage-clamped at −20 mV) expressing NR1/NR2A NMDA receptors. Top trace, response to 3 μM glutamate (+50 μM glycine). Middle trace, response of the same oocyte to the same concentration of glutamate (and glycine) but coapplied with 100 nM NVP-AAM077. There is a clear "sag" in the response before it decays to a steady-state level. Bottom trace, response of the same oocyte to the same concentration of glutamate (and glycine) but after the preapplication and equilibration of 100 nM NVP-AAM077. In this response, the current is slower to rise, no sag is observed, but the final steady-state level of the current is similar to that seen in the middle trace. B, plot illustrating the steady-state level of responses ($n = 9$) evoked by 3 μM glutamate (+50 μM glycine) when it is either coapplied or preapplied with NVP-AAM077. Responses have been normalized to the steady-state current obtained in the absence of NVP-AAM077. No significant differences in the steady-state levels of the current are observed ($p = 0.18$). C, examples of TEVC responses from an oocyte (voltage-clamped at −30 mV), expressing NR1/NR2A NMDA receptors, in response to 30 μM glutamate (+50 μM glycine) in the absence of NVP-AAM077 or in the presence of 30 nM, 300 nM, or 3 μM NVP-AAM077. D, mean inhibition curves to determine the IC_{50} of NVP-AAM077 acting at NR1/NR2A NMDA receptors and obtained when either 3 μM glutamate (+50 μM glycine; ●) or 30 μM glutamate (+50 μM glycine; ■) was used to activate NR1/NR2A NMDA receptors. Values of the IC_{50} for NVP-AAM077 were significantly different ($p < 0.001$) and were 31 ± 2 nM (for 3 μM glutamate; $n = 12$) and 215 ± 10 nM (for 30 μM glutamate; $n = 10$).

Results

NVP-AAM077 Is a Potent Antagonist of NR1/NR2A NMDA Receptor-Mediated Responses. We first investigated whether the extent of steady-state antagonism produced by NVP-AAM077 was dependent on whether this antagonist was coapplied with glutamate or preapplied so as to establish equilibrium of antagonist-receptor occupancy (Weitlauf et al., 2005). Figure 1A shows TEVC traces obtained from an experiment where we compared the extent of the steady-state inhibition produced by 100 nM NVP-AAM077 on responses evoked by 3 μM glutamate (top trace) when it was either coapplied (middle trace) with glutamate or applied 2 min before glutamate (bottom trace). As can be seen, when antagonist and agonist are coapplied, the time course of the current shows an initial "peak", which then decays to a steady-state level, whereas preincubation of the oocyte with NVP-AAM077 gives a current that rises slowly to a steady-state level. The initial peak to the current seen when agonist and antagonist are coapplied is similar to that observed previously (Weitlauf et al., 2005); however, it is most easily explained by the fact that an equilibrium of agonist and antagonist occupancy has not been established and therefore is dependent on diffusion and the association (and dissociation) rates of both ligands. Such measurements of peak responses are therefore difficult to interpret, and in our study we report only values for the steady-state level of inhibition produced by NVP-AAM077. In contrast to the study of Weitlauf et al. (2005), we did not observe any significant difference in the extent of steady-state inhibition produced by NVP-AAM077 when it was applied using either protocol. Thus, when coapplied 100 nM NVP-AAM077 + 3 μM glutamate gave responses that were 24.8 $\pm$ 2.5% of control responses (3 μM glutamate), whereas preapplication of 100 nM NVP-AAM077 followed by 3 μM glutamate application in the continued presence of the antagonist gave responses that were 27.7 $\pm$ 2.0% of control responses (n = 9; $p > 0.15$, Student's paired t test; Fig. 1B).

To assess the potency of NVP-AAM077, we constructed concentration-response curves for this antagonist by examining its ability to block NR1/NR2A NMDA receptor-mediated currents evoked by two different concentrations of glutamate. The concentrations chosen represented the EC_{50} and 10 times the EC_{50} concentrations (3 and 30 μM, respectively) of glutamate and which we have determined previously for this receptor combination (Chen et al., 2005). Figure 1C shows representative TEVC current traces obtained from an oocyte expressing NR1/NR2A NMDA receptors in response to 30 μM glutamate (alone, left-hand trace), and three traces obtained in the presence of increasing concentrations of NVP-AAM077 (30 nM–3 μM). The mean data obtained from all recordings in this series of experiments are shown in Fig. 1D and illustrate clearly that the IC_{50} for NVP-AAM077 is dependent on the glutamate concentration used to activate the NMDA receptors. Thus, responses evoked by the EC_{50} concentration of glutamate (3 μM) are half-inhibited by NVP-AAM077 at a concentration of 31 $\pm$ 2 nM (n = 12), whereas responses evoked by a higher concentration of glutamate (30 μM) are half-inhibited by NVP-AAM077 at a concentration of 214 $\pm$ 10 nM (n = 10). This dependence of the antagonist IC_{50} on the agonist concentration is, of course, entirely expected of a competitive antagonist and indeed may account for some of the differences reported in IC_{50} values of NVP-AAM077 (Neyton and Paoletti, 2006).

Determination of the Equilibrium Constant for NVP-AAM077 at NR1/NR2A NMDA Receptors. As demonstrated above, the determination of an IC_{50} value of an antagonist is critically dependent on the concentration of the agonist that is used to evoked responses. Although methods have been devised to convert IC_{50} values to equilibrium constants [for example, the Cheng-Prusoff (1973) equation], these methods are not satisfactory; furthermore, they do not give any indication as to the sort of block (competitive or noncompetitive) produced by the antagonist. Thus, to establish that NVP-AAM077 is indeed a competitive NMDA receptor antagonist and to determine its equilibrium constant, we used the method described by Schild (Arunlakshana and Schild, 1959).

Figure 2A shows a series of two-point dose-response curves that were obtained from an experiment designed to calculate dose ratios. The concentrations of glutamate chosen to obtain the "control" two-point dose-response curve are considerably less than the glutamate EC_{50} and therefore, as is predicted from the limit of the Hill equation, give a straight line on a log-log plot (see *Materials and Methods*). As can be seen in the presence of increasing concentrations of NVP-AAM077,

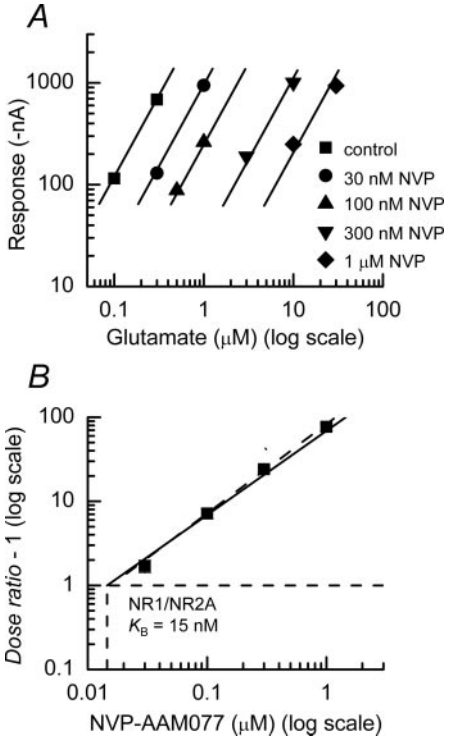

Fig. 2. Schild analysis of NVP-AAM077 action at NR1/NR2A NMDA receptors. A, example of partial, low-concentration, glutamate dose-response curves used to estimate dose ratios and obtained from an oocyte expressing NR1/NR2A NMDA receptors. The slope of the fitted line to the control responses (no NVP-AAM077; ■) was constrained and used to fit the responses obtained in the presence of 30 nM (●), 100 nM (▲), 300 nM (▼), and 1 μM (◆) NVP-AAM077. B, Schild plot for antagonism of NR1/NR2A NMDA receptors by NVP-AAM077 using dose ratios estimated from a series experiments (n = 9) such as that illustrated in A. The dashed line represents a free fit of the data and has a slope of 1.06 $\pm$ 0.05. This was considered not to be significantly different from 1, and the solid line is the fit of the data points to the Schild equation (i.e., the slope of this line is unity). The intercept on the abscissa (where the $\log_{10}$ value of the dose ratio equals 0) gives a K_B value for NVP-AAM077 of 15 nM.

these two-point dose-response curves are shifted to the right, but they remain parallel to each other. Estimates of dose-ratios at different concentrations of NVP-AAM077 from this and other experiments ($n = 9$) were obtained and used to generate the Schild plot shown in Fig. 2B. The slope of the dashed line shown in Fig. 2B is 1.06 ± 0.05, which is not significantly different from 1; therefore, the data were refitted (solid line) with the slope constrained to unity (i.e., the Schild equation) and give a mean value K_B of 15 ± 2 nM.

The Point Mutation NR2A(T671A) Causes a Reduction in NVP-AAM077 Potency. Inasmuch as agonist and (competitive) antagonist binding sites overlap, it might be expected that mutations that are known to disrupt the ability of glutamate to bind to NR2 NMDA receptor subunits may also alter the potency of competitive NMDA receptor antagonists (for review, see Chen and Wyllie, 2006; also see Anson et al., 1998; Laube et al., 2004; Chen et al., 2005). We therefore examined the effects of two-point mutations, known to reduce glutamate potency at NR2A-containing NMDA receptors (Anson et al., 1998; Chen et al., 2005), on their ability to alter the potency of NVP-AAM077. Figure 3A shows a schematic linear representation of an ionotropic glutamate receptor subunit. The ligand binding domain of such subunits is formed by amino acids located in the S1 region (located between the amino terminal domain and the first membrane-associated region) and the S2 region (located between the third and fourth membrane-associated regions). In all glutamate binding subunits, a conserved serine-threonine motif is found in the S2 domain, and both of these amino acids are known, from crystallographic studies (Furukawa et al., 2005) and supported by data from functional studies (for review, see Chen and Wyllie, 2006; also see Anson et al., 1998; Chen et al., 2004, 2005), to be directly involved in hydrogen bonding with glutamate when it occupies the binding pocket. The partial sequence (and alignment) of residues found in the S2 ligand binding domain is shown below the linear representation of the receptor subunit. Numbering of amino acids is according to their location in the mature protein (i.e., without the signal peptide).

We examined the effect of NVP-AAM077 potency on two-point mutations—the first in which the serine residue at position 670 was replaced by a glycine residue, referred to as NR2A(S670G), and the second where the threonine residue at position 671 was replaced by an alanine residue, NR2A(T671A). These mutations reduce glutamate potency such that the EC_{50} for glutamate acting at NR1/NR2A(S670G) NMDA receptors is approximately 400 μM (Chen et al., 2005; Wyllie et al., 2006), whereas the EC_{50} for glutamate acting at NR1/NR2A(T671A) NMDA receptors is around 3 mM (Anson et al., 1998). Thus, we chose these EC_{50} concentrations of glutamate to evoke responses when we constructed inhibition curves for NVP-AAM077 acting at

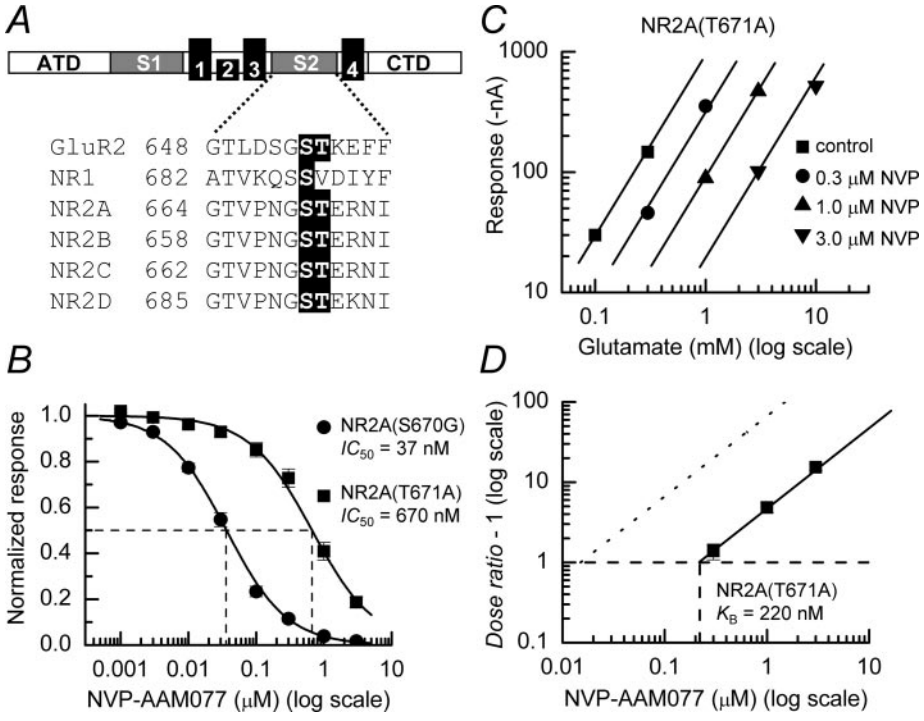

Fig. 3. Antagonism by NVP-AAM077 at NMDA receptors carrying point mutations in the ligand binding site. A, cartoon scheme depicting the topology of a glutamate receptor subunit and partial amino acid sequence of the S2 ligand binding domain of GluR2, NR1, and NR2A–NR2D receptor subunits. The conserved serine and threonine residues are highlighted. B, mean inhibition curves to determine the IC_{50} of NVP-AAM077 acting at NR1/NR2A(S670G) NMDA receptors (●) or NR1/NR2A(T671A) (■). Responses were evoked by the respective EC_{50} concentration of glutamate acting at either receptor combination [400 μM for NR1/NR2A(S670G) or 3 mM for NR1/NR2A(T671A]. The values obtained for the IC_{50} of NVP-AAM077 acting at NR1/NR2A(S670G) NMDA receptors were not significantly different from those obtained for NR1/NR2A(WT) NMDA receptors, whereas the NR2A(T671A) mutation causes a significant reduction in NVP-AAM077 potency compared with NR1/NR2A NMDA receptors ($p < 0.001$). C, example of partial, low-concentration, glutamate dose-response curves used to estimate dose ratios and obtained from an oocyte expressing NR1/NR2A(T671A) NMDA receptors. The slope of the fitted line to the control responses (no NVP-AAM077; ■) was constrained and used to fit the responses obtained in the presence of 300 nM (●), 1 μM (▲), and 3 μM (▼) NVP-AAM077. D, Schild plot for antagonism of NR1/NR2A(T671A) NMDA receptors by NVP-AAM077 using dose ratios estimated from a series experiments ($n = 8$) such as that illustrated in C. The solid line is the fit of the data points to the Schild equation (i.e., the slope of this line is unity). The intercept on the abscissa gives a K_B value for NVP-AAM077 of 220 nM. For ease of comparison, the dotted line shows the line (illustrated in Fig. 2B) that was fitted to the data obtained for NR1/NR2A NMDA receptors.

these mutated receptors. As illustrated in Fig. 3B, the IC_{50} for NVP-AAM077 at NR1/NR2A(S670G) NMDA receptors is 37 ± 2 nM (n = 9) and is not significantly different from the IC_{50} value obtained when NVP-AAM077 antagonized glutamate responses at wild-type NR2A containing NMDA receptors when these are evoked by the EC_{50} concentration of glutamate (Fig. 1D). However, we observed that NVP-AAM077 potency was reduced at NR1/NR2A(T671A) NMDA receptors. We estimated the IC_{50} of NVP-AAM077 at this receptor combination to be 670 ± 60 nM (n = 9), which is significantly different from the IC_{50} of NVP-AAM077 of 31 ± 2 nM at wild-type NR2A-containing NMDA receptors ($p < 0.001$).

We examined further the action of NVP-AAM077 at T671A-containing NMDA receptors by carrying out Schild analysis to determine its K_B at this receptor combination. Figure 3C shows representative two-point dose-response curves obtained in the absence of and in the presence of three different concentrations of NVP-AAM077 (0.3–3 μM). The lines fitted to the data points have been constrained to be parallel to each other to allow estimates of dose ratios to be obtained (see *Materials and Methods*). The Schild plot from a series (n = 8) of experiments is illustrated in Fig. 3D. A free fit of the data gave a slope value that was considered not to be different from 1; therefore, the line fitted to the data points has its slope constrained to be equal to unity (see *Materials and Methods*) and gives a value for the K_B of 220 ± 10 nM. This value is significantly greater than obtained for NVP-AAM077 of 15 ± 2 nM acting at wild-type NR2A NMDA receptors (Fig. 2B; $p < 0.001$).

NVP-AAM077 Potency at NR1/NR2B NMDA Receptors. Next, we studied the effects of NVP-AAM077 at NR1/NR2B NMDA receptors to determine whether, as has been suggested previously, this antagonist is able to discriminate between NR2A- and NR2B-containing NMDA receptors to an extent that will allow it to be a useful pharmacological tool when studying NMDA receptor function. We confirmed that the pharmacology normally expected with NR1/NR2B receptors was obtainable under our experimental recording conditions. Thus, 3 μM ifenprodil caused NR1/NR2B receptor-mediated responses (evoked by 3 μM glutamate) to be reduced to 11.9 ± 1.1% (n = 7) of control values, whereas NR1/NR2A receptor-mediated responses were not altered by 3 μM ifenprodil, being 98.9 ± 1.5% of control values (n = 6; data not shown).

Estimates of the EC_{50} for glutamate acting at NR1/NR2B NMDA receptors range from 0.5 to 5 μM (for review, see Erreger et al., 2004; also see Priestley et al., 1995; Varney et al., 1996; Laube et al., 1997, 2004; Banke and Traynelis, 2003; Neyton and Paoletti, 2006). Nonetheless, we constructed concentration-response curves for glutamate acting at this NMDA receptor subtype so that we could be confident that we would be comparing the actions of NVP-AAM077 at NR2B-containing NMDA receptors under similar levels of glutamate activation as we had done for NR2A-containing NMDA receptors. Figure 4A shows the mean concentration-response curve for glutamate-evoked NR1/NR2B NMDA receptor-mediated responses and gives an EC_{50} of 1.52 ± 0.11 μM (n = 10). Thus, we chose to determine IC_{50} values for NVP-AAM077 under conditions where NR1/NR2B NMDA receptor-mediated responses were evoked by 1.5 and 15 μM glutamate. Figure 4B illustrates the mean inhibition curves generated. For responses evoked by 1.5 μM glutamate, the IC_{50} for NVP-AAM077 was 215 ± 13 nM (n = 14), whereas when 10 times this glutamate concentration was used to activate NR1/NR2B NMDA receptors, we obtained an IC_{50} for NVP-AAM077 of 2.2 ± 0.14 μM (n = 8). The values for the IC_{50} of NVP-AAM077 acting at NR1/NR2B NMDA receptors are significantly greater than the corresponding IC_{50} values (31 and 214 nM, respectively) obtained at NR2A-containing NMDA receptors ($p < 0.001$).

To determine whether NVP-AAM077 acted as a competitive antagonist at NR2B-containing NMDA receptors, we carried out Schild analysis. Figure 4C shows examples of two-point dose-response curves obtained in the absence of and in the presence of three different concentrations of NVP-AAM077 (0.3–3 μM). As with our other experiments, the lines fitted to the data points have been constrained to be parallel to each other to allow estimates of dose ratios to be obtained. The Schild plot obtained from pooling data from a series (n = 14) of experiments is illustrated in Fig. 4D. A free fit of the data gave a slope value of 1.02 ± 0.04, which was considered not to be different from 1; therefore, the line fitted to the data points has its slope constrained to be equal to unity and gives a value for the K_B of 78 ± 3 nM. This value is significantly greater than that obtained for NVP-AAM077 acting at wild-type NR2A NMDA receptors (Fig. 2B; $p < 0.001$).

Inhibition of NMDA-Evoked Currents by NVP-AAM077. Determination of antagonist K_B values using the Schild method is independent of the nature of the agonist used to evoke responses and is one of the strengths of this method of analysis. The same is not necessarily true when determining IC_{50} values, because not only are these values dependent on the agonist concentration, as demonstrated above, but also they could be dependent on the particular agonist used to activate the receptor population. We examined the ability of NVP-AAM077 to antagonize NR1/NR2A and NR1/NR2B NMDA receptor-mediated currents evoked by NMDA itself. Concentration-response curves for NMDA (Supplemental Fig. 1A) at these two receptor subtypes gave estimates of its EC_{50} value of 64 ± 2 μM (NR1/NR2A; n = 6) and 42 ± 4 μM (NR1/NR2B; n = 6). These EC_{50} values are in agreement with estimates published previously for these receptor subtypes (Banke and Traynelis, 2003; Chen et al., 2005). Next, we determined IC_{50} values for NVP-AAM077 acting at NR1/NR2A and NR1/NR2B NMDA receptors when these receptors were activated by 50 μM NMDA (+50 μM glycine). This concentration approximates to its EC_{50} concentration for both subtypes and additionally is in the range typically used in biochemical studies of NMDA receptor function. As was the case for glutamate-evoked currents, the IC_{50} values for NVP-AAM077 (Supplemental Fig. 1B) acting at NR1/NR2A and NR1/NR2B NMDA receptors differed significantly ($p < 0.001$) and were 16 ± 2 nM (NR1/NR2A; n = 8) and 302 ± 18 nM (NR1/NR2B; n = 8). Thus, under these conditions NVP-AAM077 shows a greater degree of selectivity for NR2A-containing NMDA receptors.

Antagonism by NVP-AAM077 Is Surmountable. Competitive antagonists, by definition, result in parallel shifts in concentration-response curves but importantly they do not decrease the maximal response that can be achieved (provided sufficient agonist is present). However, because the experiments described above used low agonist concentrations

to estimate shifts in dose-response curves with NVP-AAM077, it could be argued that if this antagonist caused a depression in the maximal response, then it would be missed. Figure 5 illustrates data from experiments in which we confirmed that it was possible to obtain a maximal response in the presence of NVP-AAM077 by increasing the glutamate concentration. A maximum response (steady state, indicated by the dashed line) was obtained from an oocyte expressing NR1/NR2A NMDA receptors by applying a saturating concentration of glutamate (100 μM; Fig. 5A, left-hand trace). The recording solution was then switched to a solution that contained a high concentration of NVP-AAM077 (3 μM, i.e., 200 times the K_B), and increasing concentrations of glutamate were applied to determine whether it was possible to obtain a similar response that had been observed in the absence of the antagonist. As can be seen in Fig. 5A in the presence of 3 μM NVP-AAM077 and 3 mM glutamate, a response with a similar magnitude to that obtained under control (no NVP-AAM077) is achieved. Figure 5B shows the mean results obtained from a series of experiments ($n = 5$) examining NVP-AAM077 action at NR1/NR2A NMDA receptors. Similar experiments were also carried on oocytes expressing NR1/NR2B NMDA receptors. In these experiments ($n = 5$) the NVP-AAM077 concentration was increased to 15 μM (again so as to be approximately 200 times the K_B). The mean data from such experiments are shown in Fig. 5C and indicate that NVP-AAM077 block of NR2B-containing NMDA receptors can be overcome by applying increasing amounts of glutamate. These results together with the Schild analysis indicate that at both NR1/NR2A and NR1/NR2B NMDA receptors, NVP-AAM077 acts as a reversible competitive antagonist.

Discussion

NVP-AAM077 Is a Potent NMDA Receptor Agonist with Modest Selectivity for NR1/NR2A NMDA Receptors. Our data confirm that NVP-AAM077 is more potent at antagonizing NR1/NR2A NMDA receptor-mediated responses compared with those mediated by NR1/NR2B NMDA receptors and therefore are in general agreement with previously published work (Auberson et al., 2002; Feng et al., 2004; Liu et al., 2004; Berberich et al., 2005; Weitlauf et al., 2005; Neyton and Paoletti, 2006). However, by comparing NVP-AAM077 action at these two receptor subtypes under conditions where they are equally activated and by determining the equilibrium binding constants by Schild analysis, we have shown that the extent by which this antagonist is able to discriminate between NR2A- and NR2B-containing NMDA receptors is small (~5-fold if K_B values are compared or ~7- to 10-fold difference in IC_{50} values). As mentioned above, NVP-AAM077 shows more selectivity (in terms of

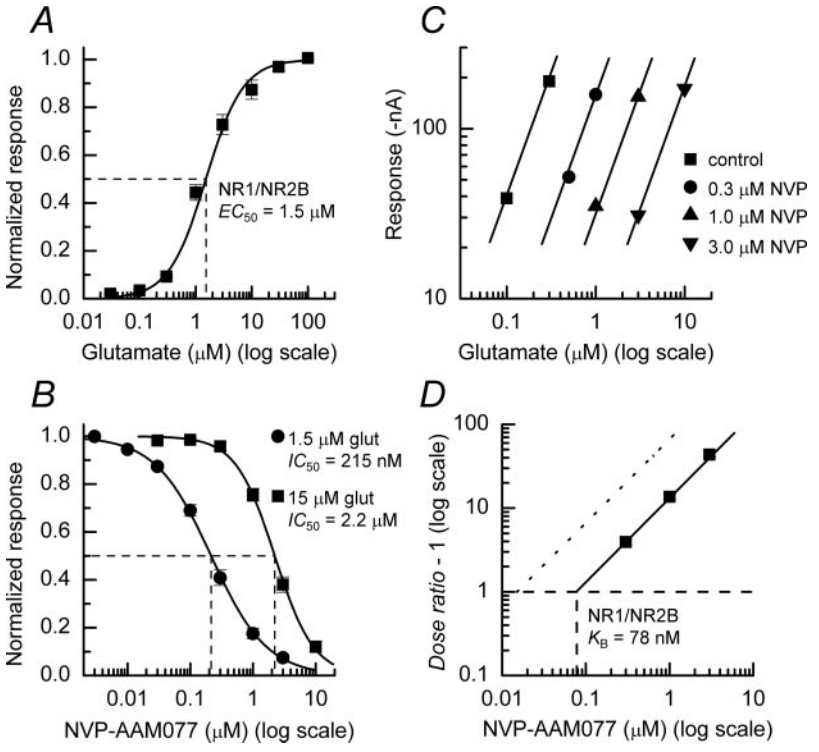

Fig. 4. NVP-AAM077 antagonism at NR1/NR2B NMDA receptors. A, mean concentration-response curve ($n = 10$) for glutamate acting at NR1/NR2B NMDA receptors. Data points are fitted with the Hill equation, which gives an estimate of the EC_{50} of 1.52 ± 0.11 μM, with a slope value of 1.32 ± 0.06. B, mean inhibition curves to determine the IC_{50} of NVP-AAM077 acting at NR1/NR2B NMDA receptors and obtained when either 1.5 μM glutamate (+50 μM glycine; ●) or 15 μM glutamate (+50 μM glycine; ■) was used to activate NR1/NR2B NMDA receptors. Values of the IC_{50} for NVP-AAM077 were significantly different ($p < 0.001$) and were 215 ± 13 nM (for 1.5 μM glutamate; $n = 14$) and 2.2 ± 0.14 μM (for 15 μM glutamate; $n = 8$). C, example of partial, low-concentration, glutamate dose-response curves used to estimate dose ratios and obtained from an oocyte expressing NR1/NR2B NMDA receptors. The slope of the fitted line to the control responses (no NVP-AAM077; ■) was constrained and used to fit the responses obtained in the presence of 300 nM (●), 1 μM (▲), and 3 μM (▼) NVP-AAM077. D, Schild plot for antagonism of NR1/NR2B NMDA receptors by NVP-AAM077 using dose ratios estimated from a series experiments ($n = 14$) such as that illustrated in C. The solid line is the fit of the data points to the Schild equation (i.e., the slope of this line is unity). The intercept on the abscissa gives a K_B value for NVP-AAM077 of 78 nM. For ease of comparison, the dotted line shows the line (illustrated in Fig. 2B) that was fitted to the data obtained for NR1/NR2A NMDA receptors.

differences in IC_{50} values) for NR2A- compared with NR2B-containing NMDA receptors when responses are evoked by NMDA rather than glutamate. Compared with the prototypical NMDA receptor antagonist, D-2-amino-5-phosphonopentanoic acid (D-AP5; see Supplemental Fig. 2), our data show that NVP-AAM077 acting at NR1/NR2A NMDA receptors is around 30-fold more potent than D-AP5, and at NR1/NR2B NMDA receptors it is around 17-fold more potent than D-AP5 [D-AP5: K_B = 460 nM (NR2A) and 1.36 μM (NR2B)]. In addition, it is interesting to note that, like NVP-AAM077, D-AP5 shows some selectivity for NR1/NR2A over NR1/NR2B NMDA receptors (~3-fold if K_B values are compared or ~5-fold difference in IC_{50} values). Thus, the structural features responsible for the increased sensitivity of NR2A-containing NMDA receptors to D-AP5 may also contribute to the increased potency of NVP-AAM077 at this receptor subtype.

Our results with NVP-AAM077 are in contrast to those obtained by both Auberson et al. (2002) and Liu et al. (2004) where they reported a >100-fold difference in IC_{50} values for a study on human recombinant NMDA receptors expressed in oocytes. Our data, however, are in excellent agreement with the recent study of Neyton and Paoletti (2006), where they, like us, examined NVP-AAM077 action at rodent NMDA receptor subtypes at equivalent levels of receptor activation (also see Feng et al., 2004). It could be argued that differences in the species chosen for study may account for these discrepancies. However, given that the amino acids that are thought to hydrogen-bond with glutamate when it occupies the ligand binding site are identical (Monyer et al., 1992; Hess et al., 1996) in rats and humans and that there is >98% amino acid sequence identity in their S1 and S2 binding regions (the site of action of NVP-AAM077), then this explanation is perhaps unlikely. More likely, and has been pointed out by Neyton and Paoletti (2006), is that differences in the concentrations of glutamate used to evoke responses at each receptor subtype might have contributed to the variation in IC_{50} values obtained. Nevertheless without a comparison between rodent and human NMDA receptors made under equivalent recording conditions it remains a possibility that NVP-AAM077 action at NMDA receptor subtypes shows a species dependence. Notwithstanding, this study is the first to report equilibrium constants for NVP-AAM077 action at NR1/NR2A and NR1/NR2B NMDA receptors and to demonstrate that its action is indeed competitive in nature and is surmountable by increasing the concentration of glutamate used to activate receptors. In addition, our results show that at least one of the residues (Thr671) that interacts directly with glutamate in the ligand binding domain (for review, see Chen and Wyllie, 2006; also see Anson et al., 1998, 2000; Chen et al., 2004, 2005; Furukawa et al., 2005) also influences NVP-AAM077 binding. The NR2A(T671A) mutation has previously been shown to reduce D-AP5 potency (Anson et al., 1998), suggesting that this residue plays an important role in competitive antagonist binding as well as agonist binding in NR2A NMDA receptor subunits.

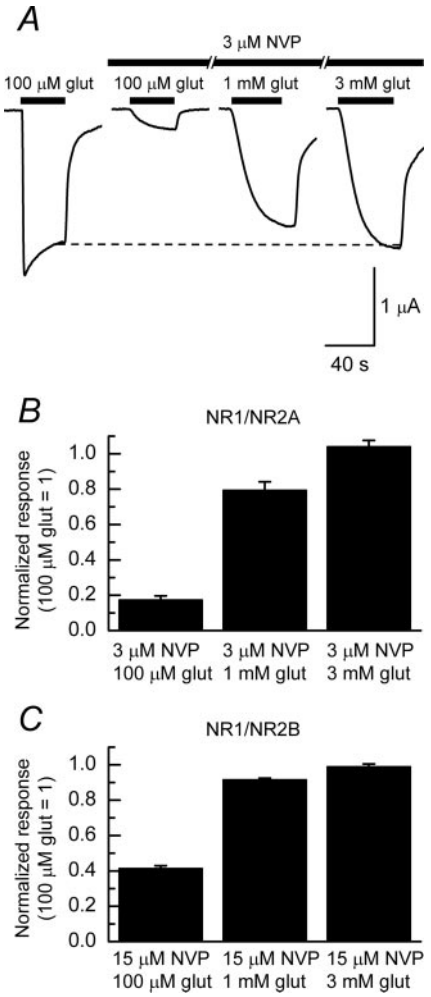

Fig. 5. NVP-AAM077 antagonism at NR1/NR2A and NR1/NR2B NMDA receptors is surmountable. A, examples of TEVC traces recorded from an oocyte, voltage-clamped at −25 mV, and expressing NR1/NR2A NMDA receptors. Increasing the concentration of glutamate from 100 μM to 3 mM in the presence of 3 μM NVP-AAM077 results in a similar maximum steady-state response (indicated by the dashed line) to that obtained with the application of 100 μM glutamate alone. B and C, bar graphs showing mean data obtained from recordings (of the sort illustrated in A) from oocytes expressing either NR1/NR2A (B; n = 5) or NR1/NR2B (C; n = 5) NMDA receptors.

NVP-AAM077 Is Predicted to Block Potently "Synaptic" Activation of Both NR1/NR2A and NR1/NR2B NMDA Receptors. So far, we have considered NVP-AAM077 actions under conditions where this antagonist is in equilibrium with both the agonist (glutamate) and the NMDA receptor population (i.e., in the steady state). However during synaptic transmission the glutamate concentration decays rapidly (within a few milliseconds) and glutamate binding to NMDA receptors does not establish equilibrium. In addition, when studying the effects of antagonists on synaptic currents, antagonists are preapplied for sufficient time so as to ensure the antagonist and receptor population are in the steady state. Moreover, if the mean lifetimes of antagonist-receptor complexes are such that their durations are much longer than the rise in concentration of agonist produced during its synaptic release, then the effect of the antagonist is to reduce the proportion of receptors that are available for activation. In effect, the antagonism produced by what is considered to be a competitive antagonist under steady-state conditions is now irreversible antagonism. We have investigated whether the K_B values we have determined for NVP-AAM077 acting at NR1/NR2A and NR1/NR2B NMDA receptors are sufficiently different to allow this antagonist to distinguish between these two receptor subtypes when these receptors are activated with brief, high (i.e., synaptic-like) concentrations of glutamate.

Figure 6A shows a kinetic scheme proposed by Erreger et al. (2005a) to account for the activation of recombinant NR1/NR2A and NR1/NR2B NMDA receptors (also see Banke and Traynelis, 2003; Erreger et al., 2005b). Incorporated in the scheme are additional states (BR, B_2R, and BRA) to describe the binding of antagonist molecules (denoted by B) to the two NR2 binding sites found in NMDA receptor complexes. The results mentioned above do not give us values of the microscopic association and dissociation rate constants for NVP-AAM077 action at NMDA receptors. Although such rate constants are not needed to determine equilibrium occupancy of receptors, they are required to allow calculation of mean lifetimes for antagonist-receptor complexes. Thus in our simulation, we have assumed an association rate (k_{+B}) for NVP-AAM077 at both NR2A and NR2B subunits of 1×10^7 M^{-1} s^{-1}. Such a value is consistent with published values for this parameter obtained from studies that have examined a variety of competitive antagonists at NMDA receptors (Benveniste et al., 1990; Benveniste and Mayer, 1991). Thus, to agree with our K_B values, we fixed the dissociation rate constants (k_{-B}) for NVP-AAM077 at 0.15 and 0.78 s^{-1} for NR1/NR2A and NR1/NR2B NMDA receptors, respectively.

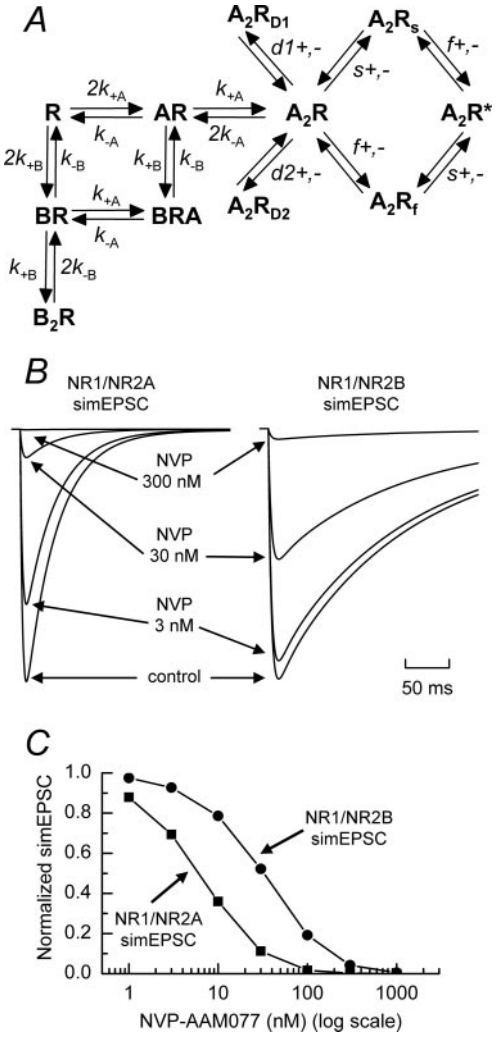

Fig. 6. Simulated EPSCs mediated by NR1/NR2A or NR1/NR2B NMDA receptors are blocked by NVP-AAM077 in an irreversible-like manner. A, kinetic scheme used to simulate NMDA receptor-mediated responses. In the reaction scheme each NR2 receptor subunit (denoted by R) can be occupied by either agonist (A) or antagonist (B). The doubly liganded A_2R state undergoes two conformation changes before channel opening (A_2R^*). These conformational changes are dependent on NR1 (fast; f) or NR2 (slow; s) gating reactions (for further details, see Banke and Traynelis, 2003; Erreger et al., 2005a,b). Two desensitized states also exist (D1 and D2). The rate constants for each reaction step were as follows: for NR2A, $k_{+A} = 2.83$ μM^{-1} s^{-1}; $k_{-A} = 31.8$ s^{-1}; $k_{D1+} = 85.1$ s^{-1}; $k_{D1-} = 29.7$ s^{-1}; $k_{D2+} = 230$ s^{-1}; $k_{D2-} = 1.01$ s^{-1}; $k_{s+} = 230$ s^{-1}; $k_{s-} = 178$ s^{-1}; $k_{f+} = 3140$ s^{-1}; $k_{f-} = 174$ s^{-1}; $k_{+B} = 10$ μM^{-1} s^{-1}; and $k_{-B} = 0.15$ s^{-1}; and for NR2B, $k_{+A} = 31.6$ μM^{-1} s^{-1}; $k_{-A} = 1010$ s^{-1}; $k_{D1+} = 550$ s^{-1}; $k_{D1-} = 81.4$ s^{-1}; $k_{D2+} = 112$ s^{-1}; $k_{D2-} = 0.91$ s^{-1}; $k_{s+} = 48$ s^{-1}; $k_{s-} = 230$ s^{-1}; $k_{f+} = 2836$ s^{-1}; $k_{f-} = 175$ s^{-1}; $k_{+B} = 10$ μM^{-1} s^{-1}; and $k_{-B} = 0.78$ s^{-1}. B, simulated (sim)EPSCs mediated by either NR1/NR2A or NR1/NR2B NMDA receptors in the absence (control) or presence (3, 30, or 300 nM) of NVP-AAM077. C, inhibition curves showing the extent of the block of the simEPSCs by NVP-AAM077 for both receptor subtypes. Note that no concentration of NVP-AAM077 selectively antagonizes the simEPSC mediated by NR1/NR2A NMDA receptors.

In the presence of NVP-AAM077 and absence of glutamate, the kinetic scheme shows that NMDA receptors can exist in one of three states: unliganded (R), singly bound with NVP-AAM077 (BR), or doubly bound (B_2R). Using the rate constants documented above, the mean lifetime of the B_2R state for NR1/NR2A NMDA receptors is 3333 ms, whereas for NR1/NR2B receptors it is 641 ms. Thus, on a synaptic time scale, there is insufficient time for NVP-AAM077 to dissociate completely to allow glutamate binding. Similar arguments can be made concerning the lifetime and occupancy of the BR state (and indeed, the BRA state when agonist is present). Thus, preapplying NVP-AAM077 reduces, in effect, the population of NMDA receptors that can be activated (on a synaptic time scale). The consequences of this for the amplitudes of synaptic currents mediated by NR1/NR2A and NR1/NR2B NMDA receptors in the presence of NVP-AAM077 are illustrated in Fig. 6, B and C. The "irreversible-like" antagonism of these simulated EPSCs by NVP-AAM077 also gives rise to an (apparent) increase in the potency of this drug, by a factor of approximately 3-fold. Thus, as shown in Fig. 6C, no concentration of NVP-AAM077 blocks NR1/NR2A NMDA receptor-mediated EPSCs without also having a significant effect on NR1/NR2B NMDA receptor-mediated EPSCs.

NVP-AAM077 has been used in studies investigating which NMDA receptor subtypes are responsible for the changes in synaptic strength that occur after the induction of long-term potentiation (Liu et al., 2004; Massey et al., 2004; Berberich et al., 2005; Weitlauf et al., 2005), and we considered whether tetanic activation of the two NMDA receptor subtypes might be affected to different extents by NVP-AAM077. The results of a Monte-Carlo simulation where a population of either 1000 NR1/NR2A or 1000 NR1/NR2B NMDA receptors are activated by a 100-Hz tetanus lasting 0.5 s (see *Materials and Methods*) in the absence or presence of NVP-AAM077 are shown in Fig. 7, A and B. Figure 7C shows the total charge transfer during the tetanus for both receptor subtypes, and although our simulation suggests that the extent of the block produced by NVP-AAM077 will be greater at NR1/NR2A than NR1/NR2B NMDA receptors (as would be expected given the differences in the K_B values), there is still considerable block of the NR1/NR2B NMDA receptor-mediated current. For example, with 300 nM NVP-AAM077, the total charge through NR1/NR2A NMDA receptors is reduced from 525.7 to 3.3 pC (99.4% block), but through NR1/NR2B NMDA receptors it is also reduced substantially from 157.7 to 23.1 pC (85.4% block). Although our simulation suggests that concentrations of NVP-AAM077 in

this range will result in considerable block of NR2B-containing NMDA receptors, it is not clear whether the concentration of ligands such as NVP-AAM077 at synaptic sites (in brain slice preparations) is equivalent to the concentration that is "bath-applied". Such differences may account for the experimental observations that ifenprodil-sensitive components to EPSCs exist in the presence of high (400 nM) concentrations of NVP-AAM077. Nevertheless, the study of Berberich et al. (2005) showed that in hippocampal slices prepared from "NR2A knockout" mice that 400 nM NVP-AAM077 produces approximately 60% block of an NR2B NMDA receptor-mediated synaptic current. Given the uncertainties of the concentrations of NVP-AAM077 reaching synaptic sites, we feel that our simulations are in agreement with data obtained from studies of synaptically localized NMDA receptors.

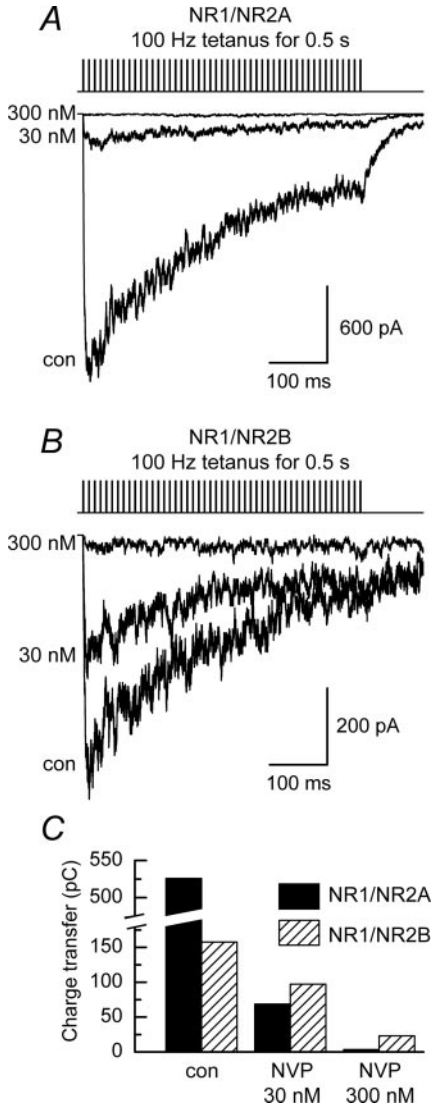

Fig. 7. Tetanic activation of NR1/NR2A or NR1/NR2B NMDA receptors is blocked potently by NVP-AAM077. A, simulated response mediated by NR1/NR2A NMDA receptors to a 100-Hz stimulus for 0.5 s (10 mM glutamate step change in concentration for 1 ms) generated in the absence of NVP-AAM077 (con) or in the presence of NVP-AAM077 at the concentrations indicated. B, simulated responses mediated by NR1/NR2B NMDA receptors generated under the same conditions as in A. C, histogram showing the effects of NVP-AAM077 on the total charge passed by either NR1/NR2A or NR1/NR2B NMDA receptors during the 100-Hz tetanus. For NR1/NR2A NMDA receptors, the charge decreases from 525.7 pC (control) to 68.6 pC (30 nM NVP-AAM077) and 3.3 pC (300 nM NVP-AAM077). For NR1/NR2B NMDA receptors, the corresponding values are 157.7 pC (control), 97.2 pC (30 nM), and 23.1 pC (300 nM).

Summary. In conclusion, NVP-AAM077 is a very potent, competitive NMDA receptor antagonist, but its selectivity for NR1/NR2A compared with NR1/NR2B NMDA receptors is such that it is not sufficient to distinguish these receptor subtypes on this pharmacological basis alone. When considering its action at synaptically activated NMDA receptors, our modeling suggests that the potency of NVP-AAM077 displayed at both NR1/NR2A and NR1/NR2B NMDA receptors means that NVP-AAM077 can be considered to act in an irreversible-like manner and will, at the concentrations commonly used (400 nM), block both receptor subtypes by more than 97%. Although our simulations of synaptic currents are based on the kinetic schemes derived from single-channel studies of recombinant (rather than native) NMDA receptors, they do allow for certain predictions of NVP-AAM077 action. Thus, where NVP-AAM077 has been used to identify specific roles played by NR2A- or NR2B-containing NMDA receptors in, for example, the induction of long-term potentiation or long-term depression (Liu et al., 2004; Massey et al., 2004; but see Berberich et al., 2005; Toyoda et al., 2005; Weitlauf et al., 2005) or in studies of NMDA receptor signaling cascades (Kinney et al., 2006; Li et al., 2006), consideration needs to be made as to whether the substantial receptor block that is predicted to occur at both receptor subtypes complicates (or alters) the interpretation of such studies.

Acknowledgments

We thank Dr. Yves Auberson for the generous gift of NVP-AAM077 and Dr. Stephen Traynelis for supplying us with NR2B cDNA. We thank Professor John S. Kelly for constructive and critical comments on the manuscript and members of the D.J.A.W. laboratory for helpful discussions and contributions.

References

Anson LC, Chen PE, Wyllie DJA, Colquhoun D, and Schoepfer R (1998) Identification of amino acid residues of the NR2A subunit that control glutamate potency in recombinant NR1/NR2A NMDA receptors. *J Neurosci* **18:**581–589.

Anson LC, Schoepfer R, Colquhoun D, and Wyllie DJA (2000) Single-channel analysis of an NMDA receptor possessing a mutation in the region of the glutamate binding site. *J Physiol (Lond)* **527:**225–237.

Arunlakshana O and Schild HO (1959) Some quantitative uses of drug antagonists. *Br J Pharmacol Chemother* **14:**48–57.

Auberson YP, Allgeier H, Bischoff S, Lingenhoehl K, Moretti R, and Schmutz M (2002) 5-Phosphonomethylquinoxalinediones as competitive NMDA receptor antagonists with a preference for the human 1A/2A, rather than 1A/2B receptor composition. *Bioorg Med Chem Lett* **12:**1099–1102.

Banke TG and Traynelis SF (2003) Activation of NR1/NR2B NMDA receptors. *Nat Neurosci* **6:**144–152.

Barker GR, Warburton EC, Koder T, Dolman NP, More JC, Aggleton JP, Bashir ZI, Auberson YP, Jane DE, and Brown MW (2006) The different effects on recognition memory of perirhinal kainate and NMDA glutamate receptor antagonism: implications for underlying plasticity mechanisms. *J Neurosci* **26:**3561–3566.

Benveniste M and Mayer ML (1991) Structure-activity analysis of binding kinetics for NMDA receptor competitive antagonists: the influence of conformational restriction. *Br J Pharmacol* **104:**207–221.

Benveniste M, Mienville JM, Sernagor E, and Mayer ML (1990) Concentration-jump experiments with NMDA antagonists in mouse cultured hippocampal neurons. *J Neurophysiol* **63:**1373–1384.

Berberich S, Punnakkal P, Jensen V, Pawlak V, Seeburg PH, Hvalby O, and Kohr G (2005) Lack of NMDA receptor subtype selectivity for hippocampal long-term potentiation. *J Neurosci* **25:**6907–6910.

Chen PE, Geballe MT, Stansfeld PJ, Johnston AR, Yuan H, Jacob AL, Snyder JP, Traynelis SF, and Wyllie DJA (2005) Structural features of the glutamate binding site in recombinant NR1/NR2A *N*-methyl-D-aspartate receptors determined by site-directed mutagenesis and molecular modeling. *Mol Pharmacol* **67:**1470–1484.

Chen PE, Johnston AR, Mok MH, Schoepfer R, and Wyllie DJA (2004) Influence of a threonine residue in the S2 ligand binding domain in determining agonist potency and deactivation rate of recombinant NR1/NR2D NMDA receptors. *J Physiol (Lond)* **558:**45–58.

Chen PE and Wyllie DJA (2006) Pharmacological insights obtained from structure-function studies of ionotropic glutamate receptors. *Br J Pharmacol* **147:**839–853.

Cheng Y and Prusoff WH (1973) Relationship between the inhibition constant (K1) and the concentration of inhibitor which causes 50 per cent inhibition (I50) of an enzymatic reaction. *Biochem Pharmacol* **22:**3099–3108.
Dingledine R, Borges K, Bowie D, and Traynelis SF (1999) The glutamate receptor ion channels. *Pharmacol Rev* **51:**7–61.
Erreger K, Chen PE, Wyllie DJA, and Traynelis SF (2004) Glutamate receptor gating. *Crit Rev Neurobiol* **16:**187–224.
Erreger K, Dravid SM, Banke TG, Wyllie DJA, and Traynelis SF (2005a) Subunit-specific gating controls rat NR1/NR2A and NR1/NR2B NMDA channel kinetics and synaptic signaling profiles. *J Physiol (Lond)* **563:**345–358.
Erreger K, Geballe MT, Dravid SM, Snyder JP, Wyllie DJA, and Traynelis SF (2005b) Mechanism of partial agonism at NMDA receptors for a conformationally restricted glutamate analog. *J Neurosci* **25:**7858–7866.
Feng B, Tse HW, Skifter DA, Morley R, Jane DE, and Monaghan DT (2004) Structure-activity analysis of a novel NR2C/NR2D-preferring NMDA receptor antagonist: 1-(phenanthrene-2-carbonyl) piperazine-2,3-dicarboxylic acid. *Br J Pharmacol* **141:**508–516.
Fischer G, Mutel V, Trube G, Malherbe P, Kew JNC, Mohacsi E, Heitz MP, and Kemp JA (1997) Ro 25-6981, a highly potent and selective blocker of *N*-methyl-D-aspartate receptors containing the NR2B subunit. Characterization in vitro. *J Pharmacol Exp Ther* **283:**1285–1292.
Furukawa H, Singh SK, Mancussco R, and Gouaux E (2005) Subunit arrangement of and function in NMDA receptors. *Nature (Lond)* **438:**185–192.
Hess SD, Daggett LP, Crona J, Deal C, Lu CC, Urrutia A, Chavez-Noriega L, Ellis SB, Johnson EC, and Velicelebi G (1996) Cloning and functional characterization of human heteromeric *N*-methyl-D-aspartate receptors. *J Pharmacol Exp Ther* **278:**808–816.
Ishii T, Moriyoshi K, Sugihara H, Sakurada K, Kadotani H, Yokoi M, Akazawa C, Shigemoto R, Mizuno N, Masu M, et al. (1993) Molecular characterization of the family of the *N*-methyl-D-aspartate receptor subunits. *J Biol Chem* **268:**2836–2843
Kinney JW, Davis CN, Tabarean I, Conti B, Bartfai T, and Behrens MM (2006) A specific role for NR2A-containing NMDA receptors in the maintenance of parvalbumin and GAD67 immunoreactivity in cultured interneurons. *J Neurosci* **26:**1604–1615.
Laube B, Hirai H, Sturgess M, Betz H, and Kuhse J (1997) Molecular determinants of agonist discrimination by NMDA receptor subunits: analysis of the glutamate binding site on the NR2B subunit. *Neuron* **18:**493–503.
Laube B, Schemm R, and Betz H (2004) Molecular determinants of ligand discrimination in the glutamate-binding pocket of the NMDA receptor. *Neuropharmacology* **47:**994–1007.
Li S, Tian X, Hartley DM, and Feig LA (2006) Distinct roles for Ras-guanine nucleotide-releasing factor 1 (Ras-GRF1) and Ras-GRF2 in the induction of long-term potentiation and long-term depression. *J Neurosci* **26:**1721–1729.
Liu L, Wong TP Pozza MF, Lingenhoehl K, Wang Y, Sheng M, Auberson YP, and Wang YT (2004) Role of NMDA receptor subtypes in governing the direction of hippocampal synaptic plasticity. *Science (Wash DC)* **304:**1021–1024.
Mallon AP, Auberson YP, and Stone TW (2005) Selective subunit antagonists suggest an inhibitory relationship between NR2B and NR2A-subunit containing *N*-methyl-D-aspartate receptors in hippocampal slices. *Exp Brain Res* **162:**374–383.
Massey PV, Johnson BE, Moult PR, Auberson YP, Brown MW, Molnar E, Collingridge GL, and Bashir ZI (2004) Differential roles of NR2A and NR2B-containing NMDA receptors in cortical long-term potentiation and long-term depression. *J Neurosci* **24:**7821–7828.
Monyer H, Burnashev N, Laurie DJ, Sakmann B, and Seeburg PH (1994) Developmental and regional expression in the rat brain and functional properties of four NMDA receptors. *Neuron* **12:**529–540.
Monyer H, Sprengel R, Schoepfer R, Herb A, Higuchi M, Lomeli H, Burnashev N, Sakmann B, and Seeburg PH (1992) Heteromeric NMDA receptors: molecular and functional distinctions of subtypes. *Science (Wash DC)* **256:**1217–1221.
Mott DD, Doherty JJ, Zhang S, Washburn MS, Fendley MJ, Lyuboslavsky P, Traynelis SF, and Dingledine R (1998) Phenylethanolamines inhibit NMDA receptors by enhancing proton inhibition. *Nat Neurosci* **1:**659–667.
Neyton J and Paoletti P (2006) Relating NMDA receptor function to receptor subunit composition: limitations of the pharmacological approach. *J Neurosci* **26:**1331–1333.
Priestley T, Laughton P, Myers J, Le Bourdelles B, Kerby J, and Whiting PJ (1995) Pharmacological properties of recombinant human *N*-methyl-D-aspartate receptors comprising NR1a/NR2A and NR1a/NR2B subunit assemblies expressed in permanently transfected mouse fibroblast cells. *Mol Pharmacol* **48:**841–848.
Toyoda H, Zhao MG, and Zhuo M (2005) Roles of NMDA receptor NR2A and NR2B subtypes for long-term depression in the anterior cingulate cortex. *Eur J Neurosci* **22:**485–494.
Varney MA, Jachec C, Deal C, Hess SD, Daggett LP, Skvoretz R, Urcan M, Morrison JH, Moran T, Johnson EC, et al. (1996) Stable expression and characterization of recombinant human heteromeric *N*-methyl-D-aspartate receptor subtypes NMDAR1A/2A and NMDAR1A/2B in mammalian cells. *J Pharmacol Exp Ther* **279:**367–378.
Vicini S, Wang JF, Li JH, Zhu WJ, Wang YH, Luo JH, Wolfe BB, and Grayson DR (1998) Functional and pharmacological differences between recombinant *N*-methyl-D-aspartate receptors. *J Neurophysiol* **79:**555–566.
Weitlauf C, Honse Y, Auberson YP, Mishina M, Lovinger DM, and Winder DG (2005) Activation of NR2A-containing NMDA receptors is not obligatory for NMDA receptor-dependent long-term potentiation. *J Neurosci* **25:**8386–8390.
Williams K (1993) Ifenprodil discriminates subtypes of the *N*-methyl-D-aspartate receptor: selectivity and mechanisms at recombinant heteromeric receptors. *Mol Pharmacol* **44:**851–859.
Wyllie DJA, Béhé P, and Colquhoun D (1998) Single-channel activations and concentration jumps: comparison of recombinant NR1a/NR2A and NR1a/NR2D NMDA receptors. *J Physiol (Lond)* **510:**1–18.
Wyllie DJA, Johnston AR, Lipscombe D, and Chen PE (2006) Single-channel analysis of a point mutation of a conserved serine residue in the S2 ligand binding domain of the NR2A NMDA receptor subunit. *J Physiol (Lond)* **574:**477–489.

Address correspondence to: Dr. David J. A. Wyllie, Centre for Neuroscience Research, University of Edinburgh, 1 George Square, Edinburgh EH8 9JZ, UK. E-mail: dwyllie1@staffmail.ed.ac.uk